JCTC Journal of Chemical Theory and Computation

What Electronic Structures and Geometries of Carborane Mono- and *ortho*-, *meta*-, and *para*-Diradicals are Preferred?

Luis Serrano-Andrés,*,† Douglas J. Klein,‡ Paul von Ragué Schleyer,§,|| and Josep M. Oliva*,⊥

Instituto de Ciencia Molecular, Universitat de València, Apartado 22085, ES-46071 Valencia, Spain, Texas A&M University at Galveston, Galveston, Texas 77553-1675, Center for Computational Chemistry, University of Georgia, Athens, Georgia 30602, Institut für Organische Chemie der Universität Erlangen-Nürnberg, Henkestrasse 42, D-91054 Erlangen, Germany, and Instituto de Química-Física Rocasolano, Consejo Superior de Investigaciones Científicas, Serrano, 119, ES-28006 Madrid, Spain

Received May 6, 2008

Abstract: Structures, relative stabilities, singlet-triplet gaps, and the ground-state character of mono- and diradicals derived from the three icosahedral carborane cage isomers have been computed by unrestricted broken-symmetry DFT and by CASPT2 methods. Whereas the bond dissociation energies (BDE) leading to the carborane monoradicals are close to the benzene BDE, the most stable carborane radicals are derived from dissociations of hydrogens farthest away from the carbon atoms. All the monomeric carborane diradicals are determined to have singlet ground states. However, the energetic accessibility of triplet states in some of the species offers the potential of building diradical multidimensional carborane network architectures with interesting magnetic properties.

1. Introduction

Carborane clusters, proposed[1] as building-blocks in a "molecular tinkertoy" set, have emerged as candidates for the design of nanosize materials with tunable electronic, optical, and magnetic properties.[2] Icosahedral *o*-, *m*-, and *p*-carboranes are commercially available. Their 12 cage atoms, serving as anchoring points, can be connected to build linear, sheetlike, and 3D molecular architectures.[3] The ion−molecule reactions of icosahedral *o*-, *m*-, and *p*-carborane in an ion trap showed that under ultrahigh vacuum conditions carborane ions reacted sequentially with their neutral counterparts to form series of cluster-of-clusters ions, i.e. 'supercluster' ions with linear, sheetlike, and 3D networks. Such clustering reactions proceeded with elimination of carborane hydrogens *but without detachment of any skeletal boron or carbon atom*. Hence, the thermal stability of the individual carborane cages was unaltered.[4] We have shown previously[5–8] how the properties of carborane cages can be tuned by appropriate modifications. This opens new possibilities for devising promising multidimensional carborane networks, e.g., for the design of cutting-edge molecular-based magnetic nanostructures for spin electronics.[9,10]

We aim to clarify the properties of (finite) 1D, 2D, and 3D constructs, based on icosahedral *o*-, *m*-, and *p*-carboranes in order to devise new materials with potential nanotechnological applications. Even expansion of the carborane cage to more than 12 vertices is nowadays possible leading to the possibility of atom encapsulation.[11] How do charge, spin (S),[5,6] and endohedral-atom inclusion[7,8,12] (M@cage) influence their properties, both in the ground and excited states?

* Corresponding author e-mail: Luis.Serrano@uv.es (L.S.-A.) and iqrjmoe@iqfr.csic.es (J.M.O.).

† Universitat de València.

‡ Texas A&M University at Galveston.

§ University of Georgia.

|| Institut für Organische Chemie der Universität Erlangen-Nürnberg.

⊥ Consejo Superior de Investigaciones Científicas.

10.1021/ct800150h CCC: $40.75
Published on Web 06/26/2008

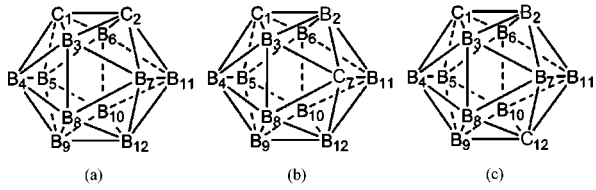

Figure 1. Labels for cage atoms in (a) *o*-carborane, (b) *m*-carborane, and (c) *p*-carborane, having point-group symmetries C_{2v}, C_{2v}, and D_{5d}, respectively. Hydrogen atoms, bound to every cage atom, are not shown for clarity.

Toward this goal, we now report a comprehensive study of the thermodynamic stabilities of carborane mono- and diradicals as well as the ground states and singlet-triplet gaps of the latter. We relate differences in behavior to their geometric and electronic peculiarities.

Previous computational investigations involved the $CB_9H_{10}^{\bullet}$ and $CB_{11}H_{12}^{\bullet}$ free radicals at the B3LYP/6−31G(d) level of theory[13] and "wheel" systems, where *closo*-carborane diradicals on opposite "poles" can either be joined to give cross-cluster bonds or can be open in singlet or triplet states.[14] The finding in the latter study that the 1,12-$C_2H_{10}B_{10}$ diradical prefers an open singlet state is confirmed and extended here. Relevant recently published experimental results include a negatively charged π-$(C_{60}^{-})_2$ dimer with a diradical state at room temperature[15] and the synthesis of dimeric diradicals derived from carborane cages connected through acetylenic and ethylenic moieties.[16]

2. Computational Methods

MP2 and B3LYP were among the methods[17] employed to compute ground states of the various carboranes radicals as well as adiabatic singlet-triplet gaps of diradical carboranes. Due to wave function instability and the need for multireference treatments, singlet state diradical geometries and energies were computed by the unrestricted (U)B3LYP broken symmetry approach (UBS),[18] an approximate but practicable method judged to be suitable for this purpose.[19] The performance of computations on selected diradicals were carefully calibrated against benchmark results employing multiconfigurational perturbation theory, CASSCF/CASPT2, a high-level method which has proven its applicability in diverse electronic structure computations.[6,7,20–28] Unless otherwise indicated, the CASPT2 multireference wave functions are based on an active space of six electrons distributed in six molecular orbitals (6,6). However smaller (2,2) and larger (12,12) active spaces were checked to ensure the stability of the results in single-point energy computations. The multiconfigurational computations used the Molcas 6.0 program[29–31] and involve CASSCF geometry optimizations and CASPT2 single-point energy computations. The 6−31G(d) basis set was employed generally. Test computations using the aug-cc-pVDZ basis sets also are discussed in order to show that increasing the size of the basis set only has minor effects. All states are described at their optimized geometries, which have been characterized as energy minima at the same level of computation through analytical second derivatives. The obtained harmonic frequencies have been used to include zero-point vibrational corrections when indicated.

3. Results and Discussion

Figure 1 displays the IUPAC numbering scheme (hydrogen atoms bound to each cage atom are not shown) for *o*-carborane, *m*-carborane, and *p*-carborane, where *o*- (*ortho*), *m*- (*meta*), and *p*- (*para*) describe the relative positions of the two carbon atoms. Single H atom removal can give five isomeric radicals from *o*-carborane, five from *m*-carborane, and two from *p*-carborane. In our designation, *r*-(*j*) is an *r*-carborane with the radical at position *j*, *j* being the lowest number among equivalent alternatives. The possible isomers are summarized below.

$$\text{Radicals derived from o} - \text{carborane} \rightarrow \{\text{o} - (1), \text{o} - (3), \text{o} - (4), \text{o} - (8), \text{o} - (9)\} \quad (1)$$

$$\text{Radicals derived from m} - \text{carborane} \rightarrow \{\text{m} - (1), \text{m} - (2), \text{m} - (4), \text{m} - (5), \text{m} - (9)\} \quad (2)$$

$$\text{Radicals derived from p} - \text{carborane} \rightarrow \{\text{p} - (1), \text{p} - (2)\} \quad (3)$$

The nomenclature scheme for diradicals is similar.

It is worth mentioning that the neutral B−H/C-H bond dissociation (homolytic bond-dissociation) is a lower energy process by 10−13 eV as compared to the ionic dissociation or deprotonation of the species derived from *o*-carborane, *m*-carborane, and *p*-carborane (see details in the Supporting Information).

3.1. Energetics of Carborane Radicals and Diradicals. The energetics of the various radicals and diradicals derived from *o*-, *m*-, and *p*-carborane (*r*-$C_2B_{10}H_{12}$, $r = o, m, p$) can be estimated from the following carbon/boron−hydrogen bond dissociation reactions (eqs 4 and 5):

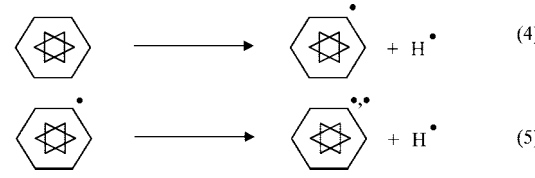

The relative energy of monoradicals (ΔE_1) and diradicals (ΔE_2) can be obtained through the corresponding relationships (eqs 6 and 7, where X represents the carborane fragment):[32]

$$\Delta E_1 = E(HX^{\bullet}) + E(H^{\bullet}) - E(HX - H) \quad (6)$$

$$\Delta E_2 = E(X^{\bullet,\bullet}) + E(H^{\bullet}) - E(HX^{\bullet}) \quad (7)$$

No experimental C−H or B−H bond dissociation energies of carboranes are available, to our knowledge. Hence, and assuming similar bonding effects in both systems, we calibrated the performance of our B3LYP/6−31G(d) level against experimental C−H bond dissociation energies (CH BDE, D_0) of benzene and the phenyl radical,[33–36] obtained from the experimental C−H bond dissociation enthalpy at 298 K (DH_{298}) and the heat capacity contribution.[36] The error in our computational level, revealed by this procedure, was corrected by evaluating eqs 6 and 7 and using an adjusted parameter, *K* (−308.05 kcal/mol or −0.490916 au), instead of the known exact energy of the hydrogen atom (−0.5 au or −313.75 kcal/mol). The value of *K* was deduced from eq 8 and experimental data[33,36]

$$\Delta E_{exp}=(D_0)_{exp}=E(C_6H_5^{\bullet})+K-E(C_6H_6)=112.4\ \text{kcal/mol} \quad (8)$$

where the computed B3LYP/6−31G(d) energy for benzene $E(C_6H_6)$ and the phenyl radical $E(C_6H_5^{\bullet})$ includes the zero-point energy (ZPE) correction. The experimental value for D_0, 112.4 kcal/mol, (eq 8) can be compared with the computed B3LYP/6−31G(d) and MP2/6−31G(d) values of 118.1 and 132.7 kcal/mol, respectively. Because of the large discrepancy, and also because the erratic behavior of the method for the diradicals, the MP2 data are disregarded in our discussion.

This procedure was used to compute the energies of all the isomeric carborane monoradicals shown comparatively in Figure 2. These derive from H atom dissociation from all distinguishable positions of the 1,2- (ortho), 1,7- (meta), and 1,12- (para) $C_2H_{12}B_{10}$ 12-vertex carborane isomers. Computations of ΔE with the basis set 6−31G(d,p) showed energy differences of only 1 kcal/mol (see the Supporting Information). The same strategy can be employed by using eq 7 to compute the three isomeric diradicals ("benzynes") derived from benzene: *ortho* (*o*-), *meta* (*m*-), and *para* (*p*-)-$C_6H_4^{\bullet,\bullet}$. Taking the corresponding experimental $(D_0)_{exp}$ values for the hydrogen dissociation leading from the phenyl radical ($C_6H_5^{\bullet}$) to the corresponding benzyne (r-$C_6H_4^{\bullet,\bullet}$), we have

$$\Delta E_{exp}^{\ r-benzyne}=(D_0)_{exp}^{\ r-benzyne}=E(r-C_6H_4^{\bullet,\bullet})+K_r-E(r-C_6H_5^{\bullet}) \quad (9)$$

The three experimental D_0 energies 76.5 (*o*-), 92.5 (*m*-), and 107.5 kcal/mol (*p*-)[34,36] were used to deduce three values of K: K_o: −324.5 kcal/mol, K_m: −308.8 kcal/mol, and K_p: −330.2 kcal/mol. These three values, employed to take into account the geometrical arrangement of the analogous diradical centers, were used in the calculations of the respective isomers of the carborane diradicals. The benzyne energies were computed at the UB3LYP/6−31G(d) level of theory for the *ortho* and *para* isomers and at the BLYP/6−31G(d) level for *meta*-benzyne. The exception for the latter was made because of the known trend of hybrid functionals to yield a highly strained bicyclic olefin structure for *meta*-benzyne instead of the correct monocyclic diradical conformation.[37,38] ZPE corrections were excluded in the calculations of the diradicals due to the poor convergence of some of the DFT broken-symmetry solutions (see below).

Figures 2 and 3 display and relate graphically the dissociation energies of the different radicals and diradicals derived from *o*-carborane, *m*-carborane, and *p*-carborane obtained by applying eqs 10 and 11

$$\Delta E_1=E(HX^{\bullet})+K-E(HX-H) \quad (10)$$

$$\Delta E_2=E(X^{\bullet,\bullet})+K_r-E(HX^{\bullet}) \quad r=o,\ m,\ p \quad (11)$$

whereas Table 1 summarizes the relative energies of the singlet carborane diradical ground states in terms of the CH or BH dissociation energies from the carborane monoradicals. Notice that some carborane diradicals can be obtained from two different consecutive H-atom abstractions; therefore, two dissociation energy values are given. For instance, *o*-(1,3)

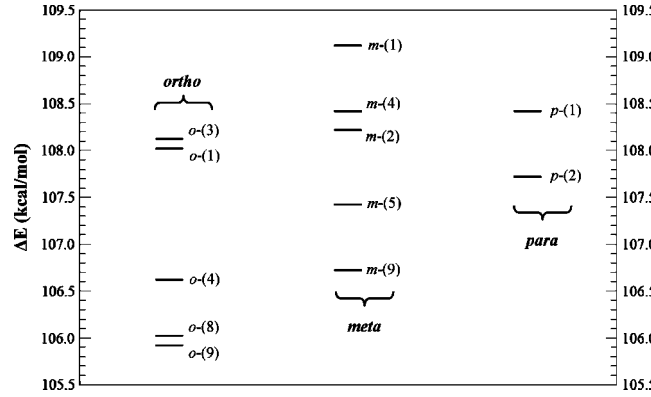

Figure 2. Comparison of the dissociation energies of monoradical derived from *o*-carborane, *m*-carborane, and *p*-carborane. ΔE computed using eq 10 at the (U)B3LYP/6−31G(d) level of theory.

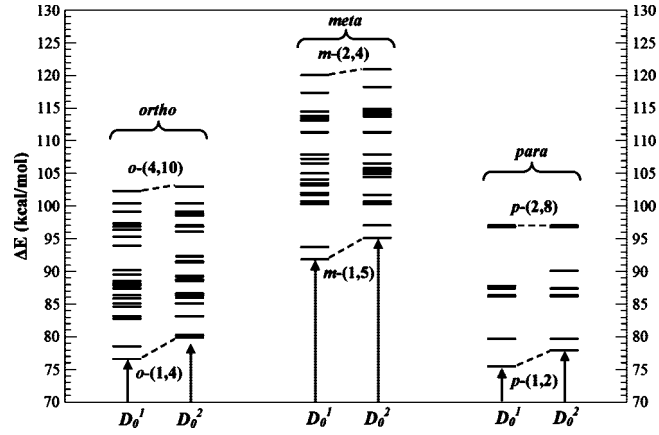

Figure 3. Plot of the dissociation energies of diradicals derived from *o*-carborane, *m*-carborane, and *p*-carborane monoradicals. ΔE computed using eq 11. Level of theory: UBS(B3LYP)/6−31G(d).

can be obtained from the radical *o*-(1) by removing the hydrogen from boron B_3 or from *o*-(3) by removing the H from carbon C_1. The energies of the carborane diradicals were based on the B3LYP broken-symmetry solution for the singlet state of the systems (see the next section), assuming, as verified by the CASPT2 calibrations, that all of them have a singlet ground state. The value for the singlet state energy was obtained by adding to the UB3LYP/6−31G(d) solution for the triplet state of the diradical the computed ΔE_{ST}(BS) singlet-triplet gap (see section 3.2).

The relative stabilities of the monoradicals (see Figure 2) obviously are influenced by the energies of the parent carboranes where the stability follows the order E(*ortho*) < E(*meta*) < E(*para*).[39] The most stable carborane radicals, with the smallest ΔEs, follow the series E(*o*-(9)) < E(*m*-(9)) < E(*p*-(2)) and correspond to the isomers where the radical center is farthest away from the cage carbons. The bond dissociation energy of the most stable radical, *o*-(9), is similar to that of the phenyl radical. In general (see Figure 3), the *para* and *meta* isomers of the carborane diradicals are the most and least stable, respectively. Structures with apical carbon atoms in the carborane cage form diradicals preferentially. Whereas the range of CH/BH monoradical bond dissociation energies is only 3 kcal/mol (Figure 2), the

Table 1. Comparison of the CH or BH Bond Dissociation Energies D_0 (in kcal/mol at the UBS(B3LYP)/6-31G(d) Level) for the Singlet Diradical Ground States Derived from *r*-Carborane Monoradicals Computed with Eqs 10 and 11[a]

diradical	D_0^1	D_0^2	diradical	D_0^1	D_0^2	diradical	D_0^1	D_0^2
o-(1,2)	84.3	84.3	*m*-(1,2)	104.4	106.8	*p*-(1,2)	76.6	79.1
o-(1,3)	79.7	81.4	*m*-(1,7)	115.0	115.0	*p*-(1,7)	88.9	91.3
o-(1,4)	77.8	81.0	*m*-(1,4)	94.9	98.2	*p*-(1,12)	87.5	87.5
o-(1,7)	95.1	98.2	*m*-(1,5)	93.0	96.3	*p*-(2,3)	80.9	80.9
o-(1,8)	88.6	92.5	*m*-(1,9)	108.4	112.5	*p*-(2,4)	97.9	97.9
o-(1,9)	83.9	87.8	*m*-(1,12)	103.2	106.5	*p*-(2,7)	88.6	88.6
o-(1,12)	85.8	89.7	*m*-(2,3)	101.5	101.5	*p*-(2,8)	98.2	98.2
o-(3,4)	89.0	90.4	*m*-(2,6)	104.7	105.6	*p*-(2,9)	87.3	87.3
o-(3,5)	98.5	99.9	*m*-(2,4)	121.2	122.1			
o-(3,6)	101.6	101.6	*m*-(2,5)	114.5	115.3			
o-(3,8)	91.4	93.5	*m*-(2,10)	114.3	116.0			
o-(3,10)	90.7	92.7	*m*-(4,8)	109.1	109.1			
o-(3,9)	97.5	99.7	*m*-(4,6)	115.6	115.6			
o-(4,5)	86.2	86.2	*m*-(4,11)	107.7	107.7			
o-(4,7)	100.3	100.3	*m*-(4,5)	102.9	102.9			
o-(4,8)	89.3	89.9	*m*-(4,12)	114.9	114.9			
o-(4,10)	103.5	104.2	*m*-(4,9)	105.2	106.1			
o-(4,9)	89.7	90.5	*m*-(4,10)	118.5	119.4			
o-(4,12)	96.5	97.2	*m*-(5,12)	112.5	112.5			
o-(8,10)	98.0	98.0	*m*-(5,10)	106.2	107.0			
o-(8,9)	87.0	87.1	*m*-(9,10)	101.9	101.9			
o-(9,12)	87.5	87.5						

[a] Two D_0's are computed for those diradicals whose parent monoradicals differ; thus, the diradical *r*-(*i*, *j*) can be derived through {*r*-(*i*) → *r*-(*i*, *j*) + H} or through {*r*-(*j*) → *r*-(*i*, *j*) + H} leading to D_0^1 and D_0^2, respectively, with $i < j$.

range for carborane diradicals is nearly ten times larger (Figure 3). Finally, it is worth mentioning that the fact that some radicals have almost degenerate energies does not imply that they coexist or interconvert at room temperature, because the corresponding conversion barrier is generally high. As an example, computations on the *o*-(8) and *o*-(9) radical show an energy barrier of about 60 kcal/mol for the 1,2-hydrogen shift. The absolute and relative energies of the ground states of the compounds used to estimate relative stabilities and an example of an interconversion barrier are included in the Supporting Information.

The electronic structures of the monoradicals have a common feature: the singly occupied molecular orbital (SOMO) corresponding to the unpaired electron in all radicals is axially delocalized—the axis corresponds to the former X-H bond at the X = B or C site where the H was removed. These SOMOs always have four nodal surfaces. Figure 4 depicts the MO ϕ_e corresponding to the unpaired electron in the radical *o*-(1) and the total spin density of the same radical. In all other species the SOMO and the spin density have very similar shapes, with ϕ_e, even for nonsymmetric radicals, having approximate axial symmetry. As expected, the spin density in the radical is largely localized around the cage atom site from which the hydrogen atom has been removed. More information about the electronic structures of the diradicals is provided below.

3.2. Electronic Structure and singlet-triplet Gaps for Carborane Diradicals. *Methodological Considerations.* Diradical systems are characterized by the existence of two electrons nominally localized at specific sites of a molecule. The energy gap between the lowest energy singlet and triplet states is governed by the effective interaction between the

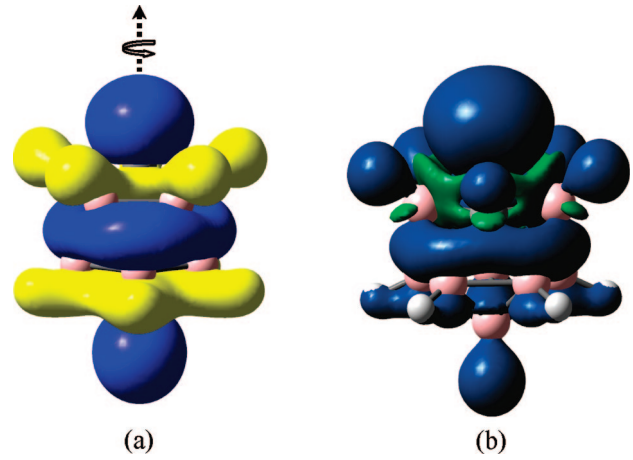

Figure 4. Electronic structure of *o*-carborane radical *o*-(1): (a) singly occupied molecular orbital (SOMO, $\phi_e = \pm 0.02$). (b) Total spin density ($\rho_s = \pm 0.0004$); the orientation of the radical corresponds to the carbon atom at the apical position (top large spin-density lobe).

electron spins of sites *i*, *j*, mapped to a Heisenberg−Dirac-Van Vleck spin Hamiltonian[40–42]

$$\hat{H}_{ex} = -J_{ij}\hat{S}_i \cdot \hat{S}_j \qquad (12)$$

Here J_{ij} is the spin-exchange coupling parameter, and a sum over *i* and *j* occurs for more than two sites. For the diradical case, J_{ij} equals the singlet-triplet splitting, with a negative value for a singlet ground state (antiferromagnetic behavior) and positive in the opposite case (ferromagnetic behavior).[19] The simplest derivations of such a spin Hamiltonian presupposes that spins are localized in each center, a phenomenon called valence trapping, but this model is often inaccurate. Still, eq 12 is generally adequate for diradicals comprised of just two unpaired electrons. For systems with several unpaired and typically delocalized valence electrons, corrections can entail further double-exchange[42,43] or cyclic (spin) permutations.[44,45] The calculation of singlet-triplet splittings, and therefore effective exchange coupling constants, J_{ij}, in almost degenerate cases by quantum chemical methods is quite delicate, requiring high accuracy to evaluate subtle correlation energy effects and to take the intrinsic multideterminantial nature of the spin manifold into account, conditions only fulfilled by computationally expensive multiconfigurational ab initio procedures with limited applicability to large complexes. A natural tendency is to move toward the widely used and less expensive Density Functional Theory (DFT) procedures.

DFT has clear limitations when applied to degenerate states, in particular because of its single-determinant character.[46,47] This circumstance occurs with diradicals, which are molecules with two weakly interacting electrons, each formally associated with different atomic centers. The standard DFT representation is approximately valid in computing triplet states but is totally inadequate for spin contaminated singlet diradicals.[19] Along with other techniques,[42] unrestricted broken symmetry (UBS) DFT approximations have been developed[18] to deal with open-shell or multiconfigurational situations. The broken spin symmetry yields a wave function which is a mixture of different spin

Table 2. Adiabatic singlet-triplet Gaps and Geometrical Parameters for Selected Carborane Diradicals at Different Levels of Theory[a]

		adiabatic singlet-triplet energy gap[b]/eV					distance between diradical centers/Å					
		B3LYP/UBS geometry		MP2 geometry		CASSCF geometry	B3LYP/UBS geometry		MP2 geometry		CASSCF geometry	
system	class	B3LYP/UBS($<S^2>$)	CASPT2	MP2	CASPT2	CASPT2	S_0	T_1	S_0	T_1	S_0	T_1
o-(1,2)	I*a*	0.93/0.93(0.00)	1.15	1.60	1.17	1.17	1.361/1.361	1.636	1.400	1.639	1.364	1.602
o-(3,6)	II*c*	−1.05/0.03(0.99)	−0.05[c]	0.19	0.03	0.06	2.800/2.880	2.887	2.892	2.885	2.899	2.901
o-(1,7)	II*b*	0.18/0.28(0.54)	−0.02[c]	0.24	−0.04[c]	0.17	2.586/2.607	2.694	2.579	2.693	2.624	2.691
o-(1,12)	III*b*	0.98/0.98(0.00)	0.85	0.99	0.87	0.76	3.097/3.097	3.090	3.100	3.101	3.121	3.118
m-(1,2)	I*a*	0.63/0.63(0.00)	0.75	0.93	0.82	0.82	1.463/1.463	1.688	1.479	1.689	1.509	1.686
m-(4,8)	I*c*	−0.01/0.38(0.75)	0.38	0.31	0.36	0.37	1.570/1.664	1.763	1.614	1.764	1.666	1.771
m-(1,7)	II*a*	−0.22/0.27(0.85)	0.36	0.94	0.33	0.37	2.292/2.462	2.517	2.432	2.517	2.438	2.517
m-(2,4)	II*c*	−0.91/-0.19(-)[e]	−0.14[c]	0.12	−0.03[c]	0.04	2.718/2.607[e]	2.838	2.837	2.843	2.842	2.855
m-(2,10)	II*c*	−0.77[d]/0.07(0.97)	−0.11[c]	0.61[d]	−0.10[c]	0.04[d]	2.707/2.806	2.819	2.793	2.828	2.853	2.840
m-(4,10)	II*c*	−0.77/-0.10(-)[e]	−0.02[c]	0.15	0.01	0.07	2.680/2.680	2.840	2.800	2.840	2.860	2.873
m-(1,12)	III*b*	0.49/0.70(0.44)	0.77	0.74	0.60	0.74	3.086/3.103	3.094	3.160	3.104	3.163	3.137
p-(1,2)	I*b*	0.91/0.91(0.00)	0.94	0.19	0.96	0.98	1.466/1.466	1.703	1.476	1.702	1.492	1.709
p-(1,7)	II*b*	−0.03/0.25(0.78)	0.27	0.24	0.22	0.34	2.454/2.596	2.663	2.378	2.669	2.615	2.659
p-(2,4)	II*c*	−0.93/-0.09(-)[e]	−0.07[c]	0.12	0.01	0.04	2.700/2.700	2.845	2.805	2.850	2.859	2.872
p-(1,12)	III*a*	0.17/0.62(0.68)	0.72	1.77	0.72	0.67	2.920/2.919	2.865	2.973	2.875	2.934	2.885
p-(2,9)	III*c*	−0.20/0.43(0.83)	0.42	1.21	0.47	0.48	3.300/3.328	3.315	3.360	3.324	3.359	3.352

[a] CASSCF computations: active space 6 electrons in 6 orbitals. [b] A positive singlet-triplet gap indicates a singlet (ground) state lower in energy. [c] At T_1 geometry the S_0 state is lower in energy than at S_0 geometry or vice versa. [d] Results increasing the basis set: B3LYP/aug-cc-pVDZ −0.71 eV; MP2/aug-cc-pVDZ 0.10 eV; CASPT2/aug-cc-pVDZ//CASSCF/6−31G(d) 0.06 eV, CASPT2(12,12)/aug-cc-pVDZ//CASSCF/6−31G(d) 0.05 eV. [e] Poor convergence. $\langle S^2 \rangle$ close to one. Less reliable result.

states.[48] singlet-triplet gaps (ΔE_{ST}) are therefore based on the standard DFT triplet state (E_T) result and the UBS (unrestricted-DFT) solution for the singlet state (E_{BS}). The gap is computed as[49]

$$\Delta E_{ST} = \frac{2(E_{BS} - E_T)}{\langle \hat{S}^2 \rangle_T - \langle \hat{S}^2 \rangle_{BS}} = \frac{2(E_{BS} - E_T)}{2 - \langle \hat{S}^2 \rangle_{BS}} \qquad (13)$$

The expression derives from a UBS calculation with a mixed wave function and considers the state of the highest multiplicity (E_T, triplet) to be a pure spin state ($\langle \hat{S}^2 \rangle_T = 2$), whereas the lower spin (E_{BS}, singlet) state, computed with the UBS method, is contaminated by higher spin state components, and its solution will not be an eigenfunction of the spin operator. The magnitude of $\langle \hat{S}^2 \rangle_{BS}$ is a measure of the degree of mixing between both states. Equation 13 is equivalent to that obtained within the spin projector technique.[42,48]

Table 2 compiles the singlet-triplet energy gaps, the expectation values for the spin operators, and the distances between diradical centers for selected carborane diradicals at different levels of theory. A positive gap indicates that the singlet (ground) state is lower in energy. Detailed discussions of the performance of the different approaches to deal with degenerate situations are available.[19] We give relevant benchmarking information regarding the level of computation employed here to obtain the energies and structures of the lowest singlet and triplet states and analyze the theoretical problems related with the diradical computations.

Results on Selected Carboranes. From the full set of carborane diradicals, Table 2 includes the different types of species identified by a nomenclature scheme. The parent *o*-, *m*-, and *p*-carboranes differ in the position of the carbon atoms. Each can give rise to different locations of the diradical centers. For instance, the carbons are adjacent in *o*-carboranes, but the radical centers can be contiguous, as in *o*-(1,2), or can be separated by one atom, *o*-(1,7), or by two atoms, *o*-(1,12). The latter has the diradical centers at opposite "poles" of the near-spherical carborane cage. We identify these three structure types as Class I, II, and III carboranes, respectively, and we combine this with labels *a*, *b*, and *c*, for diradical centers located on two carbon atoms (*a*), one carbon and one boron atom (*b*), or two boron atoms (*c*) (*cf.* Table 2).

The singlet-triplet gaps depend more on the location of the diradical centers than on any other structural parameter. For instance, at all levels of theory the computed gap in (1,2) carboranes (Classes Ia and Ib) is large (close to one eV). In such molecules, the diradical centers are contiguous, and the singlet state CASSCF wave function can be described by a predominant closed-shell electronic configuration. Consequently, standard DFT/B3LYP theory provides singlet-triplet gaps within 0.2 eV of the more accurate CASPT2 results. In contrast, the behavior of the single-reference (U)MP2 theory is erratic, deviations sometimes reach ±1 eV, essentially reflecting the large spin contamination of the unrestricted HF wave function.

The UBS results are equivalent to the standard B3LYP results for Class Ia and Ib carboranes, as expected from the single-reference character displayed by the CASSCF wave function. The expectation value of the spin operator, 0.00, indicates that the UBS solution converges to the standard B3LYP solution, with states of pure singlet spin character. Class Ic carboranes like *m*-(4,8), in which the diradical centers are two boron atoms, are different. Whereas B3LYP leads to unphysical degenerate situations, UBS and MP2 gaps are close to the CASPT2 results. The symmetry-broken (UBS) situation with $\langle \hat{S}^2 \rangle_{BS} \approx 1$ indicates diradical character. The CASPT2 gaps are quite similar to the UBS values here. The CASSCF wave function reflects a situation in which two electronic configurations are predominant, and the

Table 3. Adiabatic singlet-triplet Energy Gaps (ΔE_{ST}, eV) Computed at the Different Levels for the Singlet (S) and Triplet (T) Monomeric Diradicals Derived from *o*-, *m*-, and *p*-Carborane (See Figure 1 and Text)[a]

o-carborane	B3LYP/BS	*m*-carborane	B3LYP/BS	*p*-carborane	B3LYP/BS
label/class	ΔE_{ST}	label/class	ΔE_{ST}	label/class	ΔE_{ST}
(1,2)/Ia	0.93/0.93	(1,2)/Ib	0.63/0.63	(1,2)/Ib	0.91/0.91
(1,3)/Ib	1.07/1.07	(1,7)/IIa	−0.22/0.27	(1,7) /IIb	−0.03/0.33
(1,4)/Ib	1.07/1.07	(1,4)/Ib	1.05/1.05	(1,12) /IIIa	0.17/0.62
(1,7)/IIb	0.18/0.28	(1,5)/Ib	1.12/1.12	(2,3) /Ic	0.58/0.76
(1,8)/IIb	0.53/0.53	(1,9)/IIb	0.21/0.36	(2,4) /IIc	−0.93/−0.09[b]
(1,9)/IIIb	0.75/0.75	(1,12)/IIIb	0.49/0.70	(2,7) /Ic	−0.08/0.35
(1,12)/IIIb	0.98/0.75	(2,3)/Ic	0.73/0.83	(2,8) /IIc	−0.87/−0.11[b]
(3,4)/Ic	0.32/0.60	(2,6)/Ic	0.34/0.61	(2,9) /IIIc	−0.20/0.43
(3,5)/IIc	0.89/0.11[b]	(2,4)/IIc	−0.91/−0.19[b]		
(3,6)/IIc	−1.05/0.03	(2,5)/IIc	−0.72/0.11		
(3,8)/Ic	0.08/0.43	(2,10)/IIc	−0.77/0.07		
(3,10)/IIIc	−0.03/0.49	(4,8)/Ic	−0.01/0.38		
(3,9)/IIc	−0.58/0.13	(4,6)/IIc	−0.87/0.06		
(4,5)/Ic	0.60/0.76	(4,11)/IIIc	−0.11/0.47		
(4,7)/IIc	−0.92/0.03[b]	(4,5)/Ic	0.52/0.72		
(4,8)/Ic	0.28/0.55	(4,12)/IIc	−0.69/0.10		
(4,10)/IIc	−0.76/−0.14[b]	(4,9)/Ic	0.25/0.54		
(4,9)/Ic	0.25/0.52	(4,10)/IIc	−0.77/−0.10[b]		
(4,12)/IIc	−0.50/0.18	(5,12)/IIc	−0.51/0.21		
(8,10)/IIc	−0.67/0.11	(5,10)/Ic	0.18/0.49		
(8,9)/Ic	0.48/0.67	(9,10)/Ic	0.54/0.72		
(9,12)/Ic	0.43/0.64				

[a] A positive singlet-triplet gap indicates a singlet (ground) state lower in energy. [b] Geometry converged with lower force and displacement thresholds. Less reliable result.

HOMO (H) and LUMO (L) natural orbitals, with respective bonding and antibonding character between the contiguous boron atoms (see below), display occupations of 1.52 and 0.48 electrons, respectively. We rationalize the different behavior below based on orbital structures and interactions. However, despite the poor account of energy gaps in some cases, the computations in Table 2 indicate that the geometries obtained at the different levels of theory, B3LYP, UBS, MP2, and CASSCF, give reasonably consistent structural parameters. The single point CASPT2 gaps, based on these geometries, hardly differ more than 0.1 eV.

Class II carborane diradicals are much more interesting in terms of their potential in materials applications because of their smaller singlet-triplet gaps, especially when the diradical centers are boron atoms. Thus, Class IIc compounds like *o*-(3,6), *m*-(2,4), *m*-(2,10), *m*-(4,10), and *p*-(2,4) in Table 2 have gaps smaller than 0.1 eV at the CASSCF/CASPT2 level. Standard DFT/B3LYP theory is particularly poor in such cases. The energy of the singlet state is heavily underestimated; this leads to a negative singlet-triplet gap indicating incorrectly a triplet ground state. Errors as large as 1 eV are found. MP2 also shows erratic behavior, although increasing the one-electron basis set to aug-cc-pVDZ for *m*-(2,10) improved the results considerably (*cf.* Table 2). In contrast, UBS performs quite well compared with CASPT2 in most cases, yielding degenerate situations with small energy gaps. Except discarded computations when the wave function did not converge properly due to technical problems, singlet states always were lower in energy adiabatically. The expectation value of the spin operator for the UBS "singlet-like" solution is ≈1 for Class IIc compounds, an indication of an average mixing between the pure singlet (0.0) and triplet (2.0) cases. Analysis of the CASSCF wave function illustrates the behavior of the quantum chemical methods again. Class IIc singlet states are pure diradicals; two almost equally predominant configurations describe the wave function, and two orbitals have occupations near unity. In such situations, the UBS approach behaves much better than standard DFT, although the accuracy is, as expected, limited.[42,47] Class IIa and IIb carboranes exhibit intermediate character. Whereas the B3LYP and MP2 results are somewhat erratic, UBS gives gaps within 0.15 eV of the CASPT2 results.

The behavior of Class III carborane diradicals seems surprising at first glance. All their singlet-triplet gaps are larger than those of Class II diradicals. Class III diradicals have more stable singlet ground states, despite the larger distance found between the diradical centers (which generally favors degeneracy). This difference is rationalized below in terms of the character of the singlet state involved. The behavior of the various levels of theory with Class III carboranes is intermediate between the Class I and II behavior. Although the closed-shell HF configuration predominates in the description of the CASSCF wave function, the solution can be considered multiconfigurational. The value of the spin operator in the UBS solution reveals differences between the UBS and B3LYP descriptions. Larger deviations of the expectation value from 0.00 (see Tables 3 and 4) correspond to larger discrepancy between both UBS-DFT and DFT results. For instance, the expectation value of 0.00 for *o*-(1,12) corresponds to a singlet state well described by a closed-shell reference in the CASSCF wave function; UBS and B3LYP are equivalent. For *p*-(2,9), the UBS expectation value is $\langle \hat{S}^2 \rangle_{BS} = 0.83$, and the CASSCF wave function of the singlet state is composed of two predominant configurations: H (2.0) - L (0.0), 69%, and H (1.0) - L (1.0), 29%, with natural occupations H (1.60) and L (0.40). This intermediate diradical character, especially for

Table 4. Expectation Values for $\langle \hat{S}^2 \rangle_{BS}$ in the Broken-Symmetry BS (U)B3LYP/6-31G(d) Computations for the Singlet States of Diradical Carboranes

o-carborane	B3LYP	*m*-carborane	B3LYP	*p*-carborane	B3LYP
diradicals	$\langle S^2 \rangle$	diradicals	$\langle S^2 \rangle$	diradicals	$\langle S^2 \rangle$
(1,2)	0.00	(1,2)	0.00	(1,2)	0.00
(1,3)	0.00	(1,7)	0.85	(1,7)	0.78
(1,4)	0.00	(1,4)	0.00	(1,12)	0.68
(1,7)	0.54	(1,5)	0.00	(2,3)	0.36
(1,8)	0.00	(1,9)	0.52	(2,4)	-[a]
(1,9)	0.00	(1,12)	0.44	(2,7)	0.79
(1,12)	0.00	(2,3)	0.21	(2,8)	-[a]
(3,4)	0.55	(2,6)	0.55	(2,9)	0.83
(3,5)	-[a]	(2,4)	-[a]		
(3,6)	0.99	(2,5)	0.95		
(3,8)	0.69	(2,10)	0.97		
(3,10)	0.78	(4,8)	0.75		
(3,9)	0.94	(4,6)	0.97		
(4,5)	0.34	(4,11)	0.80		
(4,7)	-[a]	(4,5)	0.41		
(4,8)	0.58	(4,12)	0.75		
(4,10)	-[a]	(4,9)	0.60		
(4,9)	0.59	(4,10)	-[a]		
(4,12)	0.92	(5,12)	0.91		
(8,10)	0.95	(5,10)	0.64		
(8,9)	0.42	(9,10)	0.39		
(9,12)	0.46				

[a] Geometry converged with looser force and displacement thresholds. $\langle S^2 \rangle$ close to one.

Class IIIc carboranes, explains the discrepancy between the B3LYP gap (−0.20 eV) and the UBS gap (0.43 eV), the latter being quite close to the CASPT2 result (0.48 eV).

Table 3 lists the singlet-triplet (ΔE_{ST}) energy gaps for all monomeric diradicals derived from *o*-carborane, *m*-carborane, and *p*-carborane computed at the B3LYP and UBS levels of computation. The performance of different levels of theory, discussed above, leads to the conclusion that UBS results should be more trustworthy than standard B3LYP results, except when convergence is poor. The larger the gap, the closer the correspondence between both DFT-type computations. Class Ia and Ib carborane diradicals exemplify this behavior which can be rationalized by analysis of the $\langle S^2 \rangle_{BS}$ operator values (compiled in Table 4).

Only Class IIc carborane diradicals, with the diradical centers located in noncontiguous boron atoms (two connections/bonds), display degeneracy between the lowest singlet and triplet states. Such species may have interesting (temperature-dependent and readily controllable) magnetic properties. Such possibilities extend to 1D, 2D, and 3D multidimensional polyradical carborane structures with boron radical centers; exchange coupling between the different 0D units should be important. We have found no triplet diradical ground states at our highest level of theory, CASPT2//CASSCF. Therefore, it appears that all diradical *closo*-$C_2H_{10}B_{10}$ carboranes have singlet ground states.

As mentioned above, the singlet-triplet energy gaps of diradicals are generally expected to decrease as the distance (d_{XX}) between the two radical centers increases. However, the carborane diradicals Class I ($d_{XX} \approx 1.4-1.8$ Å), Class II ($d_{XX} \approx 2.5-2.8$ Å), and Class III ($d_{XX} \approx 2.9-3.4$ Å) do not behave this way. Only Class II carborane diradicals are nearly degenerate. Class III singlet-triplet gaps are greatest, despite having the largest d_{XX}'s. Clearly, the magnitude of the splitting also depends on the orbital overlap contact region of the radicaloid electron spins. As judged from the radical spin densities of Figure 4, evidently this overlap can be considerable. If the orbital overlap between the two (radical) centers were weak, then the main dependence should be that of the "exchange charge density" appearing in a traditional exchange integral, and one would anticipate a large *R (i.e.,* d_{XX} distance) dependence

$$J = J_0 e^{-\alpha R} \tag{14}$$

where α is a constant, and J_0 has a weaker polynomial dependence on R (and $1/R$) along with a possible dependence on angle of orbital orientation. Evidently, the orbital overlap is significant and may be delicately balanced with important directional dependences. Consequently, our carborane diradicals do not fulfill the rule that the exchange parameters decrease with distance. The "effective" exchange interaction is the root cause of the singlet-triplet splitting, which in turn typically dominates the magnetic properties.

Figure 5 displays the CASSCF natural HOMO- and LUMO-like orbitals of three different carborane diradicals in their lowest singlet and triplet states together with their computed ΔE_{ST} gaps. Class I carboranes have their two diradical centers on neighboring atoms. Such structures have short d_{XX} distances and large orbital overlap, which maximizes the singlet-triplet splitting. The diradical centers in Class II carboranes are on noncontiguous (two connections/bonds) atoms. Not only is the distance (d_{XX}) greater than in Class I but also the orbital overlap is smaller. Although the diradical centers in Class III carboranes, on opposite sides of the cage, are furthest apart, the orbital overlap is through the cage (the "antipodal effect")[50] and is quite large. The nature of the lowest singlet state is important. It is clearly multiconfigurational in Class I and III carboranes; the orbital occupation numbers indicate the mixed localized-delocalized character of their wave function. This can be analyzed best in Class Ic carboranes, when the diradical centers are two contiguous boron atoms. Class Ia carboranes with contiguous carbon "diradical" centers form a C═C double bond; in *o*-(1,2) the C═C distance is 1.361 Å at the DFT level. The distance between contiguous B−B diradical centers in Class Ic compounds ranges between 1.593 Å for *m*-(2,3) to 1.666 Å in *p*-(2,7) at the UBS level. These values are similar to the CASSCF distances (e.g., 1.664 Å (UBS) and 1.666 Å (CASSCF) for *m*-(4.8)) but are nearly 0.1 Å longer than the B3LYP values. The computed bond length falls within the range 1.56−1.68 Å determined as the distance of a boron−boron double bond in recently synthesized stable diborenes.[51] In Class Ic carboranes with contiguous boron radical centers, the nature of the bonding is complex. This is shown by the shape of the "HOMO" (bonding B−B) and "LUMO" (antibonding) orbitals and by their natural occupation numbers, 1.53 and 0.47, respectively. On the other hand, the occupation numbers in Class II carboranes point toward a two-configurational wave function and a more clearly diradical character for both singlet and triplet states. Illustrations with Mulliken population differences and spin densities

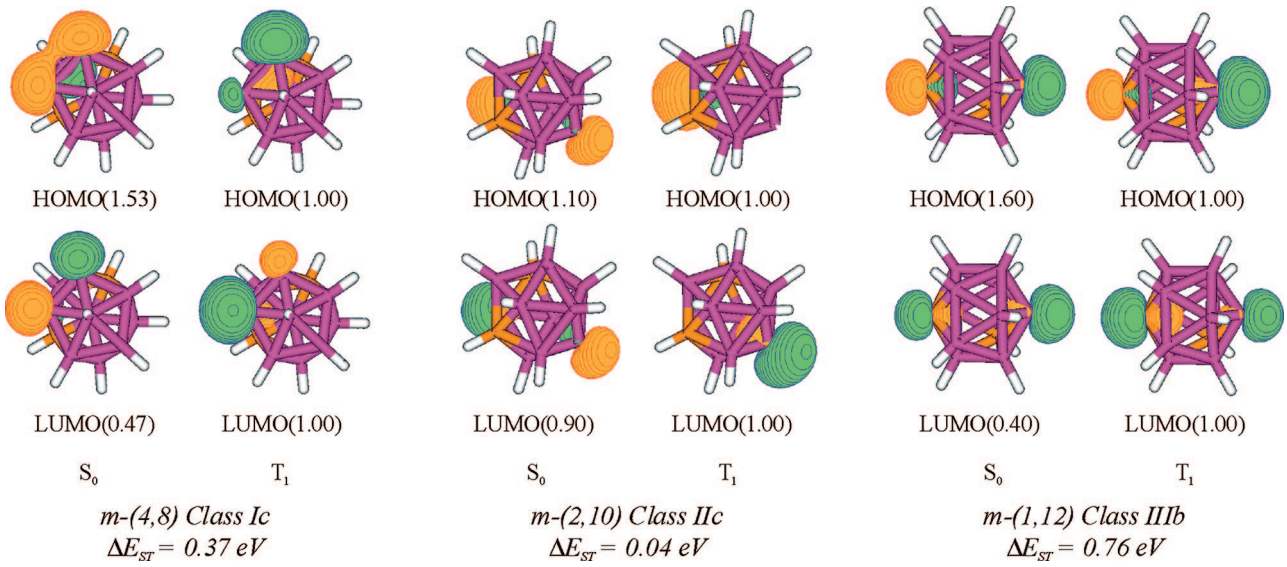

Figure 5. CASSCF HOMO- and LUMO-like natural orbital occupation for the lowest singlet and triplet states and CASPT2 singlet-triplet gaps for *m*-carborane diradical *m*-(i,j) derived from hydrogen abstraction in positions (4,8), (2,10), and (1,12).

for some of the carboranes can be found in the Supporting Information.

We conclude that it is possible to use the expectation value of $\langle \hat{S}^2 \rangle_{BS}$ in the UBS solution to evaluate the character of the singlet state, as it reflects the magnitude of the mixing between pure spin states. A value of 0.0 indicates a stable singlet wave function (identical with standard DFT), whereas a value approaching 1.0 indicates diradical character. Such systems have small HOMO−LUMO gaps and S-T separations. Thus, examples in Figure 5, the Class IIc *m*-(2,10), Class Ic *m*-(4,8), and Class IIIb *m*-(1,12) carboranes, have UBS singlet-triplet splittings of 0.07, 0.38, and 0.70 eV and expectation values for the spin operator of 0.97, 0.75, and 0.44, respectively.

4. Summary and Conclusions

A comprehensive analysis of all the isomeric monoradicals and diradicals, derived from icosahedral carboranes by single and by double hydrogen abstraction, has been presented by using high-level quantum chemical calculations. Whereas the bond dissociation energies (BDE) leading to the carborane monoradicals are close to the benzene BDE, the most stable carborane radicals (designated *o*-(9), *m*-(9), and *p*-(2)) are derived from dissociations of hydrogens farthest away from the carbon atoms. Most of the carborane radicals and diradicals will be expected to be highly reactive and only stabilized in the gas phase, having a strong tendency for dimerization or polymerization. The production of radicals as oxidized methylated carborane anions, the existence of a permethylated carborane radical less prone to dimerization,[52] and the recent synthesis of diradicals derived from the former[16] are experimental starting points of polyradical architectures based on carboranes.

The theoretical adiabatic singlet-triplet splittings for carborane diradicals underscores the possibility of using diradicals as operational magnet units in multidimensional carborane architectures. Double hydrogen abstraction from noncontiguous boron centers, particularly those separated by two connections/bonds in the carborane cages (described here as Class IIc carborane diradicals), gives rise to near degenerate lowest singlet-triplet states, although the ground state is always a singlet state at reliable levels of theory. Therefore single carborane diradicals have an antiferromagnetic behavior. Examples of Class IIc carborane diradicals are the systems *o*-(3,6) (e.g., double hydrogen abstraction from *o*-carborane in positions 3 and 6), *o*-(4,7), *m*-(2,4), *m*-(2,10), *m*-(4,10), and *p*-(2,4), in which very small singlet-triplet gaps (<0.1 eV) have been computed ($\Delta E_{ST} \approx 0.10$ eV = 2.30 kcal/mol). The performance of standard DFT, unrestricted broken-symmetry (UBS) DFT, MP2, and CASSCF/CASPT2 methods has been evaluated. UBS is the only practicable strategy giving reliable singlet-triplet gaps comparable with the more accurate but computationally demanding CASPT2 procedure. UBS may be successful because only two configurations are required to basically describe the reference wave function. Therefore, we plan to employ UBS to analyze general trends in larger diradical systems such as those with multicarborane polyradical architectures.

Additional supplemental information (geometries and frequencies) is available from the authors (PDF).

Acknowledgment. The authors would like to thank Prof. Manuela Merchán (Valencia), Prof. Wesley D. Allen (Athens), and Jose M[a] Castelló (Barcelona), for fruitful discussions and comments on the manuscript. The research was supported in Spain by projects CTQ2007-61260, MAT2006-13646-C03-02, and CSD2007-0010 Consolider-Ingenio in Molecular Nanoscience of the Spanish MEC/FEDER and in the U.S.A. by the Welch Foundation of Houston, Texas, BD-0894, and by the National Science Foundation Grant CHE-0716718.

Supporting Information Available: Mulliken population and spin densities in selected positions of several carboranes monoradicals and diradicals derived from *o*-, *m*-, and *p*- at the B3LYP/6−31G(d) level of theory, tables for the computation of relative stabilities of monoradicals and

diradicals, computed energy barrier for the 1,2-hydrogen shift in the interconversion *o*-(8) and *o*-(9) radicals (Figure S2), and figures and data on the stability of protonated carborane species. This material is available free of charge via the Internet at http://pubs.acs.org.

References

(1) Muller, J.; Base, K.; Magnera, T. F.; Michl, J. *J. Am. Chem. Soc.* **1992**, *114*, 9721.

(2) González-Campo, A.; Nuñez, R.; Viñas, C.; Boury, B. *New J. Chem.* **2006**, *30*, 546.

(3) Grimes, R. N. *J. Chem. Educ.* **2004**, *81*, 657.

(4) Hiura, H.; Kanayama, T. *J. Mol. Struct.* **2005**, *735*, 367.

(5) Oliva, J. M.; Allan, N. L.; Schleyer, P. v. R.; Viñas, C.; Teixidor, F. *J. Am. Chem. Soc.* **2005**, *127*, 13538.

(6) Oliva, J. M.; Serrano-Andrés, L. *J. Comput. Chem.* **2006**, *27*, 524.

(7) Serrano-Andrés, L.; Oliva, J. M. *Chem. Phys. Lett.* **2006**, *432*, 235.

(8) Manero, V.; Oliva, J. M.; Serrano-Andres, L.; Klein, D. J. *J. Chem. Theory Comput.* **2007**, *3*, 1399.

(9) (a) Wolf, S. A.; Awschalom, D. D.; Buhrman, R. A.; Daughton, J. M.; von Mólnar, S.; Roukes, M. L.; Chtchelkanova, A. Y.; Treger, D. M. *Science* **2001**, *294*, 1488. (b) Hirjibehedin, C. F.; Lutz, C. P.; Heinrich, A. J. *Science* **2006**, *312*, 1021. (c) Nori, F.; Tonomura, A. *Science* **2006**, *311*, 344. (d) Brune, H. *Science* **2006**, *312*, 1005.

(10) *Magnetism: Molecules to Materials*; Miller, J. S., Drillon, M., Eds.; Wiley-VCH: 2004.

(11) Ellis, D.; McIntosh, R. D.; Esquirolea, S.; Viñas, C.; Rosair, G. M.; Teixidor, F.; Welch, A. J. *Dalton Trans.* **2008**, 1009.

(12) Jemmis, E. D.; Balakrishnarajan, M. M. *J. Am. Chem. Soc.* **2000**, *122*, 7392–7393.

(13) McKee, M. L. *J. Am. Chem. Soc.* **1997**, *119*, 4220.

(14) Wang, Z. X.; Schleyer, P. v. R. *Angew. Chem., Int. Ed.* **2002**, *41*, 4082.

(15) Konarev, D. V.; Khasanov, S. S.; Otsuka, A.; Saito, G.; Lyubovskaya, R. N. *J. Am. Chem. Soc.* **2006**, *128*, 9292.

(16) Eriksson, J.; Vyakaranam, K.; Ludvík, J.; Michl, J. *J. Org. Chem.* **2007**, *72*, 2351.

(17) *Gaussian 03, Revision C.02*; Frisch, M. J.; Trucks, G. W.; Schlegel, H. B.; Scuseria, G. E.; Robb, M. A.; Cheeseman, J. R.; Montgomery, J. A.,Jr.; Vreven, T.; Kudin, K. N.; Burant, J. C.; Millam, J. M.; Iyengar, S. S.; Tomasi, J.; Barone, V.; Mennucci, B.; Cossi, M.; Scalmani, G.; Rega, N.; Petersson, G. A.; Nakatsuji, H.; Hada, M.; Ehara, M.; Toyota, K.; Fukuda, R.; Hasegawa, J.; Ishida, M.; Nakajima, T.; Honda, Y.; Kitao, O.; Nakai, H.; Klene, M.; Li, X.; Knox, J. E.; Hratchian, H. P.; Cross, J. B.; Bakken, V.; Adamo, C.; Jaramillo, J.; Gomperts, R.; Stratmann, R. E.; Yazyev, O.; Austin, A. J.; Cammi, R. ; Pomelli, C.; Ochterski, J. W.; Ayala, P. Y.; Morokuma, K.; Voth, G. A.; Salvador, P. ; Dannenberg, J. J.; Zakrzewski, V. G.; Dapprich, S.; Daniels, A. D.; Strain, M. C.; Farkas, O.; Malick, D. K.; Rabuck, A. D.; Raghavachari, K.; Foresman, J. B.; Ortiz, J. V.; Cui, Q.; Baboul, A. G.; Clifford, S.; Cioslowski, J.; Stefanov, B. B.; Liu, G.; Liashenko, A.; Piskorz, P.; Komaromi, I.; Martin, R. L.; Fox, D. J.; Keith, T.; Al-Laham, M. A.; Peng, C. Y.; Nanayakkara, A.; Challacombe, M.; Gill, P. M. W.; Johnson, B.; Chen, W.; Wong, M. W.; Gonzalez, C.; Pople, J. A. Gaussian, Inc.: Wallingford, CT, 2004.

(18) (a) Yamaguchi, K.; Yoshioka, Y.; Takayuki, F. *Chem. Phys. Lett.* **1977**, *46*, 360. (b) Noodleman, L. *J. Chem. Phys.* **1981**, *74*, 5737. (c) Borden, W. T.; Davidson, E. R.; Feller, D. *Tetrahedron* **1982**, *38*, 737. (d) Noodleman, L.; Davidson, E. R. *Chem. Phys.* **1986**, *109*, 131. (e) Noodleman, L.; Peng, C. Y.; Case, D. A.; Mouesca, J. M. *Chem. Rev.* **1995**, *144*, 199. (f) Yamaguchi, K.; Kawasaki, T.; Takano, Y.; Kigarawa, Y.; Yamashita, Y.; Fujita, H. *Int. J. Quantum Chem.* **2002**, *90*, 370.

(19) Calzado, C. J.; Cabrero, J.; Malrieu, J. P.; Caballol, R. *J. Chem. Phys.* **2002**, *116*, 2728.

(20) Andersson, K.; Malmqvist, P.; Roos, B. O. *J. Chem. Phys.* **1992**, *96*, 1218.

(21) Serrano-Andrés, L.; Merchán, M.; Nebot-Gil, I.; Lindh, R.; Roos, B. O. *J. Chem. Phys.* **1993**, *98*, 3151.

(22) Roos, B. O.; Andersson, K.; Fülscher, M. P.; Malmqvist, P.; Serrano-Andrés, L.; Pierloot, K.; Merchán, M. *Adv. Chem. Phys.* **1996**, *93*, 219.

(23) Borin, A. C.; Serrano-Andrés, L. *Chem. Phys.* **2000**, *262*, 253.

(24) Serrano-Andrés, L.; Merchán, M.; Borin, A. C. *Proc. Natl. Acad. Sci. U.S.A.* **2006**, *103*, 8691.

(25) Serrano-Andrés, L.; Fülscher, M. P.; Roos, B. O.; Merchan, M. *J. Phys. Chem.* **1996**, *100*, 6484.

(26) Serrano-Andrés, L.; Forsberg, N.; Malmqvist, P.-Å. *J. Chem. Phys.* **1998**, *108*, 7202.

(27) Muñoz, D.; De Graaf, C.; Illas, F. *J. Comput. Chem.* **2004**, *25*, 1234.

(28) Serrano-Andrés, L.; Merchán, M.; Borin, A. C. *Chem. Eur. J.* **2006**, *12*, 6559.

(29) Andersson, K.; Barysz, M. ; Bernhardsson, A.; Blomberg, M. R. A.; Carissan, Y.; Cooper, D. L.; Cossi, M.; Fülscher, M. P.; Gagliardi, L.; de Graaf, C.; Hess, B.; Hagberg, G.; Karlström, G.; Lindh, R.; Malmqvist, P.-Å.; Nakajima, T.; Neogrády, P.; Olsen, J.; Raab, J.; Roos, B. O.; Ryde, U.; Schimmelpfennig, B.; Schütz, M.; Seijo, L.;Serrano-Andrés, L.; Siegbahn, P. E. M.; Stålring, J.; Thorsteinsson, T.; Veryazov, V.; Widmark, P.-O. MOLCAS, version 6.0; Department of Theoretical Chemistry, Chemical Centre, University of Lund: Lund, Sweden, 2004.

(30) Karlström, G.; Lindh, R.; Malmqvist, P.-Å.; Roos, B. O.; Ryde, U.; Veryazov, V.; Widmark, P.-O.; Cossi, M.; Schimmelpfennig, B.; Neograd y, P.; Seijo, L. *Comput. Mater. Sci.* **2003**, *28*, 222.

(31) Veryazov, V.; Widmark, P.-O.; Serrano-Andŕes, L.; Lindh, R.; Roos, B. O. *Int. J. Quantum Chem.* **2004**, *100*, 626.

(32) Nonhebel, D. C.; Tedder, J. M.; Walton, J. C. *Radicals*; Cambridge University Press: Cambridge, 1979.

(33) Ervin, K. M.; DeTuri, V. F. *J. Phys. Chem. A* **2002**, *106*, 9947.

(34) Wenthold, P. G.; Squires, R. R. *J. Am. Chem. Soc.* **1994**, *116*, 6401.

(35) G. E. Davico, V. M.; Bierbaum, C. H.; DePuy, G. B.; Ellison, R. R. Squires. *J. Am. Chem. Soc.* **1995**, *117*, 2590.

(36) Blanksby, S. J.; Ellison, G. B. *Acc. Chem. Res.* **2003**, *36*, 255.

(37) Winkler, M.; Sander, W. *J. Phys. Chem. A* **2001**, *105*, 10422.

(38) Schreiner, P. R.; Navarro-Vazquez, A.; Prall, M. *Acc. Chem. Res.* **2005**, *38*, 29.

(39) *Gmelin Handbuch Der Organische Chemie*; Ergenzungswerek zur 8, Auflage, Band Berlin-Heidelberg, Seite 15, 1977.

(40) Eq 12 corresponds to a purely phenomenological Hamiltonian.

(41) (a) Heisenberg, W. Z. *Phys.* **1928**, *49*, 619. (b) Dirac; P, A. M. *Proc. R. Soc. London, Ser. A* **1929**, *123*, 714. (c) Van Vleck, *J. Phys. Rev.* **1934**, *45*, 405.

(42) Ciofini, I.; Daul, C. A. *Coord. Chem. Rev.* **2003**, *238*, 187.

(43) Klein, D. J.; Seitz, W. A. *Phys. Rev. B* **1973**, *8*, 2236.

(44) Mulder, J. J. C.; Oosterhoff, L. *J. Chem. Commun.* **1970**, 305.

(45) Wu, J.; Schmalz, T. G.; Klein, D. J. *J. Chem. Phys.* **2002**, *117*, 9977.

(46) Parr, R. G.; Young, W. *Density Functional Theory of Atoms and Molecules*;Oxford University Press: New York, 1989.

(47) Bersuker, I. B. *J. Comput. Chem.* **1997**, *18*, 260.

(48) Ovchinnikov, A.; Labanowski, J. K. *Phys. Rev. A* **1996**, *53*, 3946.

(49) Noodleman, L., Jr. *J. Chem. Phys.* **1979**, *70*, 4903.

(50) Bühl, M.; Schleyer, P. v. R.; Havlas, Z.; Hnyk, D.; Hermanek, S. *Inorg. Chem.* **1991**, *30*, 3107.

(51) (a) Wang, Y.; Quillian, B.; Wei, P.; Wannere, C. S.; Xie, Y.; King, R. B.; Schaefer, H. F., III; Schleyer, P. v. R.; Robinson, G. H. *J. Am. Chem. Soc.* **2007**, *129*, 12412. (b) Wang, Y. Z.; Quillian, B.; Wei, P. R. *J. Am. Chem. Soc.* **2008**, *130*, 3298.

(52) King, B. T.; Noll, B. C.; McKinley, A. J.; Michl, J. *J. Am. Chem. Soc.* **1996**, *118*, 10902.

CT800150H